Journal of Sound and Vibration (1997) **208**(1), 73–99

APPLICATION OF AN ASYMPTOTIC METHOD TO TRANSIENT DYNAMIC PROBLEMS

M. Fafard, K. Henchi and G. Gendron

GIREF, Department of Civil Engineering, Laval University, Quebec, G1K 7P4 Canada

and

S. Ammar

Pratt & Whitney Canada, 1000 Marie-Victorin, Longueuil, Quebec, Canada J4G 1A1

(*Received* 10 *July* 1996, *and in final form* 20 *June* 1997)

A new method to solve linear dynamics problems using an asymptotic method is presented. Asymptotic methods have been efficiently used for many decades to solve non-linear quasistatic structural problems. Generally, structural dynamics problems are solved using finite elements for the discretization of the space domain of the differential equations, and explicit or implicit schemes for the time domain. With the asymptotic method, time schemes are not necessary to solve the discretized (space) equations. Using the analytical solution of a single degree of freedom (DOF) problem, it is demonstrate, that the Dynamic Asymptotic Method (DAM) converges to the exact solution when an infinite series expansion is used. The stability of the method has been studied. DAM is conditionally stable for a finite series expansion and unconditionally stable for an infinite series expansion. This method is similar to the analytical method of undetermined coefficients or to power series method being used to solve ordinary differential equations. For a multi-degree-of-freedom (MDOF) problem with a lumped mass matrix, no factorization or explicit inversion of global matrices is necessary. It is shown that this conditionally stable method is more efficient than other conditionally stable explicit central difference integration techniques. The solution is continuous irrespective of the time segment (step) and the derivatives are continuous up to order N-1 where N is the order of the series expansion.

1. INTRODUCTION

The so-called perturbation technique or asymptotic method has been known for more than a century [1]. It has been used to find the solution of a problem through an asymptotic development which is a function of an independent parameter a:

$$\{\mathbf{u}(a)\} = \sum_{j=0}^{N} a^j\{\mathbf{u}_j\} = \{\mathbf{u}_0\} + a\{\mathbf{u}_1\} + a^2\{\mathbf{u}_2\} + \cdots + a^N\{\mathbf{u}_N\}, \tag{1}$$

where the vectors $\{\mathbf{u}_j\}$ are independent of the variable a. This technique, for example, has been applied to discover the planet Neptune by the French astronomer Leverrier. His computations were based on the perturbation of the orbit of Uranus. In the same manner, the planet Pluton has been discovered using a perturbation of the orbit of Neptune [1]. This technique has also been used in other fields. Its main drawback was related to the manipulation of the asymptotic developments. That is why this

0022–460X/97/460073 + 27 $25.00/0/sv971169

technique was limited to very low orders. Nowadays, using symbolic manipulation software, it is easier to manipulate the algebra of the asymptotic method even for very high orders.

Some researchers have adopted the asymptotic method in order to solve structural stability problems. Koiter [2] was one of the pioneers in this field and his Ph.D. thesis was on the stability of structures using the perturbation method. Thompson and Walker [3] have applied this technique, in combination with the finite element method, to the solution of non-linear problems. Their success was limited and they concluded that this method is not applicable to the development of new solution techniques. A detailed literature review can be found in the paper by Gallagher [4].

In the mid and late seventies, many remarkable developments were made by Budiansky [5] and Potier-Ferry [6]. These developments were based on Koiter's work. Apparently, the first interesting article on the application of the asymptotic method combined with finite element formulations was published by Damil and Potier-Ferry [7]. They applied it to the solution of a non-linear quasistatic problem. They called the method the *asymptotic numerical method*. Subsequently, Cochelin *et al*. [8–11] at the University of Metz, have presented many results based on this approach. They have proved that the numerical asymptotic method can be used effectively to solve elastic non-linear problems using the finite element method. In their case, the discretized equilibrium equations are written in a polynomial form.

Recently, Ammar [12] has extended the asymptotic numerical method to the case of equilibrium equations that are not based on a polynomial form (shell finite element formulations using large rotations theory). This new approach is called the *perturbed asymptotic method*. He has demonstrated that the classical numerical asymptotic and the perturbed asymptotic methods are more efficient than the classical Newton–Raphson method for the solution of a non-linear quasistatic problem.

In this paper, a new approach, called *dynamic asymptotic method* (DAM), is presented for the solution of transient dynamic problems. Using a finite element discretization scheme in space, the linear dynamic problem results in a set of ordinary differential equations of the form:

$$[\mathbf{M}]\{\ddot{\mathbf{u}}(t)\} + [\mathbf{C}]\{\dot{\mathbf{u}}(t)\} + [\mathbf{K}]\{\mathbf{u}(t)\} = \{\mathbf{F}(t)\}, \tag{2}$$

where $[\mathbf{M}]$, $[\mathbf{C}]$ and $[\mathbf{K}]$ are respectively the mass, damping and stiffness matrices, $\{\mathbf{u}\}$ the nodal displacement vector, and a dot denotes differentiation with respect to time t. At this stage, it is obvious that the use of a numerical technique to discretize the time domain is necessary. Equation (2) can be projected in the modal space using standard modal superposition techniques [13, 14]. If the full system is conserved, the time domain can be discretized using the standard Euler, second order explicit, or Newmark-β implicit schemes. In either case, the resulting discretized system can be written as

$$[\bar{\mathbf{K}}]\{\Delta\mathbf{u}\} = \{\mathbf{R}(t)\}, \qquad \{\mathbf{u}(t+\Delta t)\} = \{\mathbf{u}(t)\} + \{\Delta\mathbf{u}\}, \tag{3a, b}$$

where $[\bar{\mathbf{K}}]$ and $\{\mathbf{R}(t)\}$ are respectively the effective stiffness matrix and the effective incremental load vector. Both the definition of $[\bar{\mathbf{K}}]$ and $\{\mathbf{R}(t)\}$ depend on the integration scheme used. The vector $\{\Delta\mathbf{u}\}$ is the incremental displacement vector to be added to the known solution at time t, $\{\mathbf{u}(t)\}$, to obtain $\{\mathbf{u}(t+\Delta t)\}$. In all cases, the solution is obtained in an incremental manner which means that the nodal displacement, velocity and acceleration vectors are known only at certain points in the time domain

(0, Δt, $2\Delta t$, . . . , $n\Delta t$, etc.). Unfortunately, the explicit method is conditionally stable and very small time steps are often needed. The unconditionally stable implicit scheme permits the use of larger time steps, the size of which is governed only by accuracy considerations. Unfortunately, this scheme requires a matrix factorization which means that larger computer core storage is needed and more operations per time step are required than with the central difference scheme. Also, to avoid the aliasing phenomenon, the time step must be less than or equal to the lowest period which participates in the response divided by ten [14].

In the following sections, the solution of the transient dynamic problem using the asymptotic development equation (1) is presented. This dynamic asymptotic method (DAM) does not need any time integration scheme and is continuous for any time. If the mass matrix is diagonal, no global matrix factorization is required because the inverse of this matrix corresponds to the inverse of each individual diagonal term:

$$[M_{n\times n}]^{-1}=\begin{bmatrix} 1/M_{11} & 0 & 0 & 0\\ 0 & 1/M_{22} & 0 & 0\\ 0 & 0 & \ddots & 0\\ 0 & 0 & 0 & 1/M_{nn}\end{bmatrix}.$$

This paper focuses only on the fundamentals of the DAM (principles and stability analysis). Finally, it is demonstrated that the DAM is similar to the methods of undetermined coefficients and power series being used to solve ordinary differential equations.

2. ASYMPTOTIC DEVELOPMENT IN THE TIME DOMAIN

2.1. BASIC CONCEPT

The principle behind this new method, is to determine the nodal solution (finite element discretization of space is assumed) which is a function of time, and is expressed as a power series of order N (asymptotic development with center $t=0$):

$$\{\mathbf{u}(t)\}=\{\mathbf{u}_0\}+t\{\mathbf{u}_1\}+t^2\{\mathbf{u}_2\}+t^3\{\mathbf{u}_3\}+\cdots+t^N\{\mathbf{u}_N\},\qquad \{\mathbf{u}(t)\}=\sum_{j=0}^{N}t^j\{\mathbf{u}_j\},\quad (4a, b)$$

where $\{\mathbf{u}_j\}$ are the unknown vectors which are independent of time. From equation (4), the nodal velocities and acclerations can be written as

$$\{\dot{\mathbf{u}}(t)\}=\sum_{j=1}^{N}jt^{(j-1)}\{\mathbf{u}_j\},\qquad \{\ddot{\mathbf{u}}(t)=\sum_{j=2}^{N}j(j-1)t^{(j-2)}\{\mathbf{u}_j\}.\quad (5a, b)$$

It is observed from equations (4) and (5a) that at $t=0$, $\{\mathbf{u}_0\}$ and $\{\mathbf{u}_1\}$ represent the initial conditions (displacements and velocities) and therefore, these two vectors are assumed to be known. Now, consider the nodal load vector which is also a function of time and is defined in equation (2). Just like $\{\mathbf{u}(t)\}$, this vector can also be expressed as

$$\{\mathbf{F}(t)\}=\sum_{j=0}^{N-2}t^j\{\mathbf{F}_j\}.\quad (6)$$

The development of the loading term up to order $(N-2)$ instead of N will be explained after equation (9b) is presented. Using equations (4–6), the equations of motion (2) can be written as

$$[\mathbf{M}]\left(\sum_{j=2}^{N} j(j-1)t^{(j-2)}\{\mathbf{u}_j\}\right)+[\mathbf{C}]\left(\sum_{j=1}^{N} jt^{(j-1)}\{\mathbf{u}_j\}\right)+[\mathbf{K}]\left(\sum_{j=0}^{N} t^j\{\mathbf{u}_j\}\right)=\sum_{j=0}^{N-2} t^j\{\mathbf{F}_j\}. \quad (7a)$$

By grouping terms of similar powers of t in equation (7), the following equation is obtained:

$$\begin{aligned}
&2[\mathbf{M}]\{\mathbf{u}_2\}+[\mathbf{C}]\{\mathbf{u}_1\}+[\mathbf{K}]\{\mathbf{u}_0\}-\{\mathbf{F}_0\}+t(6[\mathbf{M}]\{\mathbf{u}_3\}+2[\mathbf{C}]\{\mathbf{u}_2\}+[\mathbf{K}]\{\mathbf{u}_1\}-\{\mathbf{F}_1\})\\
&\quad+t^2(12[\mathbf{M}]\{\mathbf{u}_4\}+3[\mathbf{C}]\{\mathbf{u}_3\}+[\mathbf{K}]\{\mathbf{u}_2\}-\{\mathbf{F}_2\})+t^3(20[\mathbf{M}]\{\mathbf{u}_5\}+4[\mathbf{C}]\{\mathbf{u}_4\}\\
&\quad+[\mathbf{K}]\{\mathbf{u}_3\}-\{\mathbf{F}_3\})+\cdots+t^{N-2}(N(N-1)\,[\mathbf{M}]\{\mathbf{u}_N\}+(N-1)\,[\mathbf{C}]\{\mathbf{u}_{N-1}\}\\
&\quad+[\mathbf{K}]\{\mathbf{u}_{N-2}\}-\{\mathbf{F}_{N-2}\})=0. \qquad (7b)
\end{aligned}$$

Since the equilibrium equations (2) must be satisfied for any value of t, one can conclude that

$$2[\mathbf{M}]\{\mathbf{u}_2\}+[\mathbf{C}]\{\mathbf{u}_1\}+[\mathbf{K}]\{\mathbf{u}_0\}=\{\mathbf{F}_0\};\qquad 6[\mathbf{M}]\{\mathbf{u}_3\}+2[\mathbf{C}]\{\mathbf{u}_2\}+[\mathbf{K}]\{\mathbf{u}_1\}=\{\mathbf{F}_1\}; \quad (8a)$$

$$\ldots;\qquad N(N-1)\,[\mathbf{M}]\{\mathbf{u}_N\}+(N-1)\,[\mathbf{C}]\{\mathbf{u}_{N-1}\}+[\mathbf{K}]\{\mathbf{u}_{N-2}\}=\{\{\mathbf{F}_{N-2}\}. \quad (8b)$$

Equations (8) represent a set of $(N-2)$ systems of equations. It should be noted that the vectors $\{\mathbf{u}_0\}$ and $\{\mathbf{u}_1\}$ are the initial conditions of the above mentioned second order problem. Thus, from equations (8), the unknown discrete spatial vectors can be written as

$$\{\mathbf{u}_2\}=\tfrac{1}{2}\,[\mathbf{M}]^{-1}(\mathbf{F}_0\}-[\mathbf{C}]\{\mathbf{u}_1\}-[\mathbf{K}]\{\mathbf{u}_0\});\qquad \{\mathbf{u}_3\}=\tfrac{1}{6}\,[\mathbf{M}]^{-1}(\{\mathbf{F}_1\}-2[\mathbf{C}]\{\mathbf{u}_2\}-[\mathbf{K}]\{\mathbf{u}_1\}) \quad (9a)$$

$$\ldots;\qquad \{\mathbf{u}_N\}=(1/N(N-1))\,[\mathbf{M}]^{-1}(\{\mathbf{F}_{N-2}\}-(N-1)\,[\mathbf{C}]\{\mathbf{u}_{N-1}\}-[\mathbf{K}]\{\mathbf{u}_{N-2}\}). \quad (9b)$$

It is seen that all vectors $\{\mathbf{u}_j\}$ are obtained in a recursive fashion from the two previous vectors $\{\mathbf{u}_{j-1}\}$ and $\{\mathbf{u}_{j-2}\}$ and the load vector $\{\mathbf{F}_{j-2}\}$. It is obvious that the accuracy of the dynamic response depends on the value of N, larger values of N resulting in higher accuracy. When a finite series of terms is used, one can determine a radius of convergence beyond which the series will diverge. Therefore, a convergence criterion must be defined in order to establish the critical time value t_{crit}, beyond which the accuracy of the solution is not satisfactory. From equation (9b), it is also noted that for computation of the last vector $\{\mathbf{u}_N\}$, the two previous vectors $\{\mathbf{u}_{N-1}\}$ and $\{\mathbf{u}_{N-2}\}$ and the vector $\{\mathbf{F}_{N-2}\}$ must be known. This explains why the time load vector is only expanded up to order $(N-2)$ instead of N.

If there exists a criterion the radius of convergence of the asymptotic expansion, the critical time t_{crit} can then be calculated. Using equations (4) and (5), the displacements and the velocities can be evaluated at t_{crit}. The expansion of a new series with center $t=t_{crit}$ can be written as

$$\{\mathbf{u}(t_{crit}+\tau)\}=\sum_{j=0}^{N}(t-t_{crit})^j\{\mathbf{u}_j\}=\sum_{j=0}^{N}\tau^j i\{\mathbf{u}_j\}, \quad (10)$$

where

$$\{\mathbf{u}_0\} = \{\mathbf{u}(\tau = 0)\} = \{\mathbf{u}(t = t_{crit})\}, \qquad \{\mathbf{u}_1\} = \{\dot{\mathbf{u}}(\tau = 0)\} = \{\dot{\mathbf{u}}(t = t_{crit})\}. \tag{11}$$

As seen from equation (11), the solution (displacements) and its first derivative (velocities) are continuous at $t = t_{crit}$. The load vector can also be written in the same manner as

$$\{\mathbf{F}(t_{crit} + \tau)\} = \sum_{j=0}^{N-2} \tau^j \{\mathbf{F}_j\}. \tag{12}$$

Finally, equation (9) is used to evaluate the new $\{\mathbf{u}_j\}$ vectors. Figure 1 illustrates this step-by-step procedure schematically.

2.2. MODE SUPERPOSITION AND DAM

Having demonstrated that DAM can be applied to solve dynamic problems with the full system of equations, it is also possible to apply DAM in modal subspace using a mode superposition technique. One calls this method, modal dynamic asymptotic method (MDAM). To develop this method, one applies the asymptotic development to each uncoupled equation resulting from the transformation to the modal space. The modal transformation can be written:

$$\{\mathbf{u}_n\} = [\mathbf{X}]\{\mathbf{y}_m\}, \qquad \{\mathbf{p}_m(t)\} = [\mathbf{X}]\{\mathbf{F}(t)\}, \qquad [\mathbf{X}]^{\mathrm{T}}[\mathbf{M}][\mathbf{X}] = [\mathbf{I}],$$
$$[\mathbf{X}]^{\mathrm{T}}[\mathbf{K}][\mathbf{X}] = [\boldsymbol{\lambda}] = [\boldsymbol{\omega}^2] \qquad \text{and} \qquad [\mathbf{X}]^{\mathrm{T}}[\mathbf{C}][\mathbf{X}] = [2\boldsymbol{\xi\omega}], \tag{13}$$

where $[\mathbf{X}]$ is the matrix of the m eigenvectors and $[\boldsymbol{\omega}^2]$ is a diagonal matrix containing the pulsation squared and $[2\boldsymbol{\xi\omega}]$ is a diagonal matrix where $\boldsymbol{\xi}$ is the modal damping. One obtains a set of uncoupled equations:

$$\ddot{y}_r + 2\omega_r \xi_r \dot{y}_r + \omega_r^2 y_r = p_r. \tag{14}$$

By using a separate asymptotic development for each equation (14):

$$y_r = \sum_{j=0}^{N} t^j y_{r(j)}, \tag{15}$$

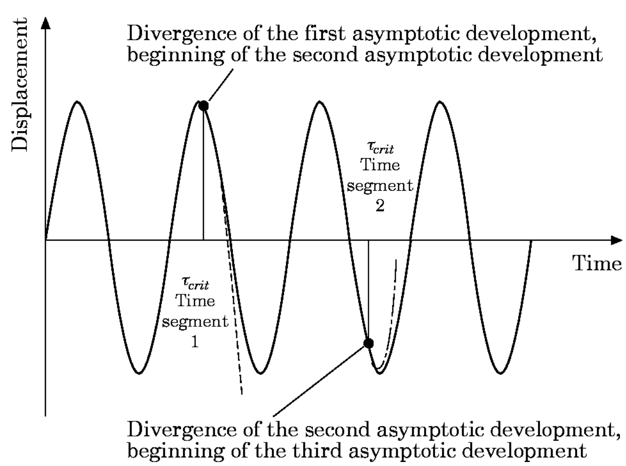

Figure 1. Step by step procedure with DAM: ——, reference solution; - - - -, first asymptotic development; –·–, second asymptotic development.

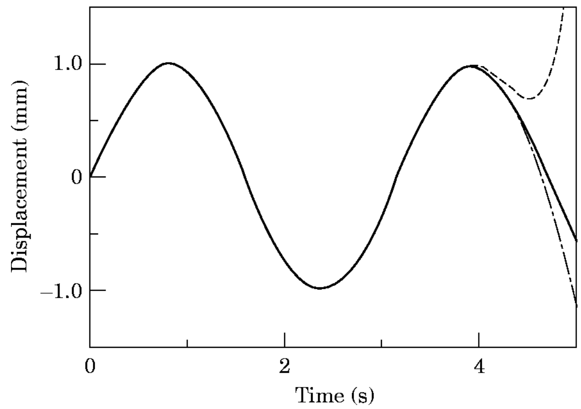

Figure 2. Time step change with dynamic asymptotic method: ——, reference solution; - - - -, solution with $(N-1)$ terms; –·–, solution with N terms.

and using the approach described in section 2.1, one can write

$$y_{r(N)} = (1/N(N-1))\,[p_{r(N-2)} - (N-1)\,(2\omega_r\,\xi_r)y_{r(N-1)} - \omega_r^2\,y_{r(N-2)}], \tag{16}$$

where the initial conditions are

$$\{\mathbf{y}_{r(0)}\} = [\mathbf{X}]^{-1}\{\mathbf{u}_0\} = [\mathbf{X}]^{\mathrm{T}}[\mathbf{M}]\{\mathbf{u}_0\}, \qquad \{\mathbf{y}_{r(1)}\} = [\mathbf{X}]^{-1}\{\mathbf{u}_1\} = [\mathbf{X}]^{\mathrm{T}}[\mathbf{M}]\{\mathbf{u}_1\}.$$

2.3. AUTOMATIC TIME SEGMENT (STEP) COMPUTATION

With the dynamic asymptotic method, it is not possible to obtain the solution with only one limited series expansion because the solution diverges for a value of t larger than t_{crit}. The series development must be within the radius of convergence of the series. Therefore, the critical time t_{crit} must be such that the given mathematical norm based on the displacement or on the equations of motion (equation (2)) is less than a fixed small value (10^{-3} to 10^{-6}). It would be time consuming to adopt a value of t_{crit} by trial and error in order to determine the norm.

In the present work, the criterion to obtain the value of t_{crit} is based on the fact that the solutions of the asymptotic developments will be approximately the same if series of order $(N-1)$ and (N) are used. The main characteristic of the polynomial series of order $(N-1)$ and N is shown in Figure 2. For order $(N-1)$, the series diverges to the upper part of the figure and for order N to the lower part. Therefore, it is observed that for a specific tolerance ε, the criterion for the selection of t_{crit} can be written as

$$\frac{\|\{\mathbf{u}(t^i_{crit}+\tau)\}_{order\ N} - \{\mathbf{u}(t^i_{crit}+\tau)\}_{order\ N-1}\|}{\|(\mathbf{u}(t^i_{crit}+\tau)\}_{order\ N} - \{\mathbf{u}(t^i_{crit})\}\|} = \frac{\|\tau^N\{\mathbf{u}_N\}\|}{\|\tau\{\mathbf{u}_1\} + \tau^2\{\mathbf{u}_2\} + \cdots + \tau^N\{\mathbf{u}_N\}\|} \leqslant \varepsilon, \tag{17a}$$

where t^i_{crit} represents the critical time of the previous time series expansion. Neglecting the higher order terms in the denominator, equation (17a) becomes

$$\tau^N\|\{\mathbf{u}_N\}\|/\tau\|\{\mathbf{u}_1\}\| \leqslant \varepsilon. \tag{17b}$$

Once vectors $\{\mathbf{u}_1\}$ and $\{\mathbf{u}_N\}$ are known, and for a given value of ε, the critical time can be estimated for the segment $(i+1)$ by the equation:

$$t^{i+1}_{crit} = (\varepsilon\|\{\mathbf{u}_1\}\|/\|\{\mathbf{u}_N\}\|)^{1/N-1}, \qquad \text{if} \qquad \|\{\mathbf{u}_1\}\| \neq 0. \tag{18a}$$

Recalling that vector $\{\mathbf{u}_1\}$ corresponds to the velocities at the end of the previous segment, it relates therefore to the initial conditions of the current time segment. In the case where $\{\mathbf{u}_1\}$ is zero, the critical time segment can be obtained by

$$t_{crit}^{i+1} = (\varepsilon \,\|\{\mathbf{u}_2\}\|/\|\{\mathbf{u}_N\}\|)^{1/N-2}. \tag{18b}$$

For the MDAM, the time segment length (critical time) to use is the one corresponding to the lowest period of vibration (or highest frequency) retained:

$$t_{crit}^{i+1} = \begin{Bmatrix} (\varepsilon |y_{r(1)}/y_{r(N)}|)^{1/N-1} & \text{if} & y_{r(1)} \neq 0 \\ (\varepsilon |y_{r(2)}/y_{r(N)}|)^{1/N-2} & \text{if} & y_{r(1)} = 0 \end{Bmatrix} \text{ for the highest frequency.} \tag{18c}$$

For the numerical examples presented in the sections 4 and 5, equation (18) is employed to determine the value of the critical time. Other techniques have been proposed by Cochelin [8] to establish the radius of convergence of the polynomial series.

2.3. REMARKS

DAM and MDAM are efficient techniques and they can easily be implemented in any finite element software. There are two approaches to compute the right side of equation (9). The matrix products $[\mathbf{C}]\{\mathbf{u}_{j-1}\}$ and $[\mathbf{K}]\{\mathbf{u}_{j-2}\}$ can be performed either at the global level or at the element level. In the former case, these two matrices must be stored in addition to the mass matrix. In the latter case, no additional computer storage is needed and each element stiffness and damping matrices must be computed $(N-2)$ times in order to determine the $(N-2)$ $\{\mathbf{u}_j\}$ vectors. If numerical integration must be performed for each element, this approach can be time consuming. If the Rayleigh damping matrix (linear combination of the mass and rigidity matrices) is used, the previous procedure can be easily modified. The DAM is similar to a step-by-step integration method but there are three major differences between these two approaches:

(1) In the DAM, no hypothesis is made on the approximation of time derivatives.
(2) The time segment in the asymptotic method can be very large and automatically computed. The time segment is defined as the difference between two consecutive critical times (t_{crit}). Thus, the time segment does not have the same meaning as the time step of the classical integration schemes. The criterion to maintain a specified level of accuracy in the solution is based only on the radius of convergence of the time series.
(3) Finally, the asymptotic procedure yields the quasi-analytical solution no matter what the value of the critical time segment between two consecutive asymptotic developments is. This is because equation (10) is continuous between two critical time values. Thus, the solution can be evaluated at any time between them.

Finally, the DAM applied to linear problems can be compared to the method of undetermined coefficients and the power series method (the analytical techniques used to solve ordinary differential linear equations [15, 16]). One knows that the solution of second order ordinary differential equations is the result of a complementary solution $u_h(t)$ and a particular solution $u_p(t)$:

$$m\,\mathrm{d}^2u/\mathrm{d}t^2 + c\,\mathrm{d}u/\mathrm{d}t + ku = f(t), \qquad u(t) = u_h(t) + u_p(t), \tag{19a, b}$$

where m, c and k are the mass, damping and stiffness of the mass–damper–spring system; $u_h(t)$ is the solution of a homogeneous differential equation ($f(t) = 0$); $u_p(t)$ is the particular solution for a non-homogeneous equation. If the load vector is defined in a polynomial form up to power N, the particular solution, which will satisfy the second order equation [15], can be written as

$$u_p(t) = u_0 + u_1 t + u_2 t^2 + u_3 t^3 + \cdots + u_N t^N, \tag{20}$$

where the u_j are the unknown coefficients. Thus, substituting equation (20) in equations (19), and expressing all terms as a power of time, the unknown coefficients can be determined. In order to establish the stability of this explicit method, is presented in the following section a stability analysis for different values of the order N.

3. STABILITY STUDY

It is well known that explicit time integration schemes are conditionally stable [17]. The DAM is an explicit method and for the method to be stable, the time segment length must satisfy a stability criterion. To determine the stability limit of the DAM, the technique described in reference [17] is used.

Since damping is small for practical structures, it can be neglected in studying the stability behavior of DAM. One assumes, without any loss of generality, that the structure is only subjected to initial conditions; no external loading is applied. Using equations (4), (5a) and (9), one can easily demonstrate that:

$$\begin{Bmatrix} \mathbf{u}^{p+1} \\ \dot{\mathbf{u}}^{p+1} \end{Bmatrix} = \begin{bmatrix} [\mathbf{A}] & [\mathbf{B}] \\ [\tilde{\mathbf{B}}] & [\tilde{\mathbf{A}}] \end{bmatrix} \begin{Bmatrix} \mathbf{u}^{p} \\ \dot{\mathbf{u}}^{p} \end{Bmatrix} = [\mathbf{S}] \begin{Bmatrix} \mathbf{u}^{p} \\ \dot{\mathbf{u}}^{p} \end{Bmatrix},$$

$$[\mathbf{A}] = \sum_{n=0}^{m_1} \frac{(\Delta t)^{2n}}{(2n)!} (-[\mathbf{M}]^{-1}[\mathbf{K}])^n, \qquad [\mathbf{B}] = \sum_{n=0}^{m_2} \frac{(\Delta t)^{2n+1}}{(2n+1)!} (-[\mathbf{M}]^{-1}[\mathbf{K}])^n,$$

$$[\tilde{\mathbf{A}}] = \sum_{n=0}^{m_2} \frac{(\Delta t)^{2n}}{(2n)!} (-[\mathbf{M}]^{-1}[\mathbf{K}])^n, \qquad [\tilde{\mathbf{B}}] = \sum_{n=1}^{m_1} \frac{(\Delta t)^{2n-1}}{(2n-1)!} (-[\mathbf{M}]^{-1}[\mathbf{K}])^n,$$

$$m_1 = \begin{cases} N/2 & \text{if } N \text{ is even,} \\ (N-1)/2 & \text{if } N \text{ is odd,} \end{cases} \qquad m_2 = \begin{cases} N/2 - 1 & \text{if } N \text{ is even,} \\ (N-1)/2 & \text{if } N \text{ is odd,} \end{cases} \tag{21}$$

where $\{\mathbf{u}^p\}$ and $\{\dot{\mathbf{u}}^p\}$ are the displacement and velocity vectors at the end of the time segment p; for $p = 0$, they represent initial conditions. The meaning of Δt in equation (21) is the time segment length corresponding to what was previously called the critical time (section 2.2). $[\mathbf{S}]$ is the amplification matrix. One can demonstrate that the system is stable if the spectral radius of $[\mathbf{S}]$ is less than or equal to one [17].

One can rewrite equations (21) in the modal space using equations (13):

$$\text{if } N \text{ is even,} \quad \begin{Bmatrix} y^{p+1} \\ \dot{y}^{p+1} \end{Bmatrix} = \left[\begin{array}{c:c} [\hat{\mathbf{A}}] + \dfrac{(\Delta t[\boldsymbol{\omega}])^N}{N!}(-1)^{N/2} & [\bar{\mathbf{B}}] \\ \hdashline -[\boldsymbol{\omega}_i^2]\,[\hat{\mathbf{B}}] & [\hat{\mathbf{A}}] \end{array} \right] \begin{Bmatrix} y^{p} \\ \dot{y}^{p} \end{Bmatrix}; \tag{22a}$$

$$\text{if } N \text{ is odd,} \quad \begin{Bmatrix} y^{p+1} \\ \dot{y}^{p+1} \end{Bmatrix} = \left[\begin{array}{c:c} [\bar{\mathbf{A}}] & -[1/\boldsymbol{\omega}_i^2]\,[\hat{\mathbf{B}}] + [1/\boldsymbol{\omega}_i]\dfrac{(\Delta t[\boldsymbol{\omega}])^N}{N!}(-1)^{N-1/2} \\ \hdashline [\hat{\mathbf{B}}] & [\bar{\mathbf{A}}] \end{array} \right] \begin{Bmatrix} y^{p} \\ \dot{y}^{p} \end{Bmatrix}, \tag{22b}$$

where matrices $[\bar{\mathbf{A}}]$, $[\bar{\mathbf{B}}]$, $[\hat{\mathbf{A}}]$ and $[\hat{\mathbf{B}}]$ are diagonal and defined by

$$\bar{A}_{ii} = \sum_{n=0}^{m_1} \frac{(\Delta t\omega_i)^{2n}}{(2n)!} (-1)^n, \qquad \bar{B}_{ii} = \sum_{n=0}^{m_2} \frac{(\Delta t\omega_i)^{2n+1}}{\omega_i\,(2n+1)!} (-1)^n,$$

$$\hat{A}_{ii} = \sum_{n=0}^{m_2} \frac{(\Delta t\omega_i)^{2n}}{(2n!)} (-1)^n, \qquad \hat{B}_{ii} = \sum_{n=1}^{m_1} \omega_i \frac{(\Delta t\omega_i)^{2n-1}}{(2n-1)!} (-1)^n. \tag{23}$$

Equation (22) represents a system of uncoupled equations. Stability analysis will be applied to one modal equation:

$$\begin{Bmatrix} y^{p+1} \\ \dot{y}^{p+1} \end{Bmatrix} = \begin{bmatrix} A_{11} & A_{12} \\ A_{21} & A_{22} \end{bmatrix} \begin{Bmatrix} y^p \\ \dot{y}^p \end{Bmatrix}. \tag{24a}$$

If N is even,

$$A_{22} = 1 - \frac{(\Delta t\omega)^2}{2!} + \frac{(\Delta t\omega)^4}{4!} - \cdots + (-1)^{N/2-1} \frac{(\Delta t\omega)^{N-2}}{(N-2)!}, \qquad A_{21} = -\omega^2 A_{12},$$

$$A_{11} = A_{22} + (-1)^{N/2} \frac{(\Delta t\omega)^N}{N!},$$

$$A_{12} = \frac{1}{\omega}\left(\frac{(\Delta t\omega)}{1!} - \frac{(\Delta t\omega)^3}{3!} + \cdots + (-1)^{N/2-1} \frac{(\Delta t\omega)^{N-1}}{(N-1)!}\right); \tag{24b}$$

if N is odd,

$$A_{11} = A_{22} = 1 - \frac{(\Delta t\omega)^2}{2!} + \frac{(\Delta t\omega)^4}{4!} - \cdots + (-1)^{(N-1)/2} \frac{(\Delta t\omega)^{N-1}}{(N-1)!},$$

$$A_{21} = -\omega\left(\frac{(\Delta t\omega)}{1!} - \frac{(\Delta t\omega)^3}{3!} + \cdots + (-1)^{(N-1)/2} \frac{(\Delta t\omega)^{N-2}}{(N-2)!},\right.$$

$$A_{12} = -\frac{1}{\omega^2} A_{21} + \frac{1}{\omega}\left((-1)^{(N+1)/2} \frac{(\Delta t\omega)^N}{(N)!}\right). \tag{24c}$$

The spectral radius of equation (24) is defined by [17]

$$\rho([\mathbf{A}]) = \max_i |\lambda_i([\mathbf{A}])|,$$

$$\lambda_{1,2} = A_1 \pm (A_1^2 - A_2)^{1/2}, \qquad A_1 = \tfrac{1}{2}\,\text{trace}\,[\mathbf{A}], \qquad \mathbf{A}_2 = \det\,[\mathbf{A}]. \tag{25}$$

If $A_1^2 < A_2$, equation (25) becomes

$$\lambda_{1,2} = A_1 \pm i(A_2 - A_1^2)^{1/2}, \qquad \rho([\mathbf{A}]) = \sqrt{(A_1)^2 + ((A_2 - A_1^2)^{1/2})^2} = \sqrt{A_2} = \sqrt{\det\,[\mathbf{A}]}. \tag{26}$$

When eigenvalues are complex conjugate (so-called super-stability case [17]), the spectral radius is one when N tends toward infinity and in this case, DAM and MDAM are unconditionally stable:

$$\lim_{N\to\infty} A_{11} = \lim_{N\to\infty} A_{22} = \cos(\omega\Delta t), \qquad \lim_{N\to\infty} A_{12} = -\lim_{N\to\infty} A_{21} = \sin(\omega\Delta t),$$

$$\lim_{N\to\infty} \rho([\mathbf{A}]) = \lim_{N\to\infty} \sqrt{\det\,[\mathbf{A}]} = 1.$$

For a finite value of N, one can easily demonstrate, for the super-stabilty case,

$$\rho([\mathbf{A}])^2 = 1 + \sum_{i=M,2}^{2N-2} (\omega \Delta t)^i \left(\frac{1}{((i/2)!)^2} + \frac{(-1)^L}{(i-N)!N!} + \left(\sum_{j=i-N+1}^{i/2-1} 2\frac{(-1)^{j+i/2}}{j!(i-j)!} \right) \right), \qquad (27)$$

where $M = N + 1$ and $L = 1 + i/2$ if N is odd and $M = N$ and $L = i/2$ if N is even. For example, for $N = 2$ to $N = 9$, the spectral radii squared are given by

$$N = 2, \qquad \rho^2 = 1 + \frac{(\omega \Delta t)^2}{2}; \qquad N = 3, \qquad \rho^2 = 1 + \frac{(\omega \Delta t)^4}{12};$$

$$N = 4, \qquad \rho^2 = 1 - \frac{(\omega \Delta t)^4}{24} + \frac{(\omega \Delta t)^6}{144};$$

$$N = 5, \qquad \rho^2 = 1 - \frac{(\omega \Delta t)^6}{180} + \frac{(\omega \Delta t)^8}{2880};$$

$$N = 6, \qquad \rho^2 = 1 + \frac{(\omega \Delta t)^6}{720} - \frac{(\omega \Delta t)^8}{2880} + \frac{(\omega \Delta t)^{10}}{86400};$$

$$N = 7, \qquad \rho^2 = 1 + \frac{(\omega \Delta t)^8}{6720} - \frac{(\omega \Delta t)^{10}}{75600} + \frac{(\omega \Delta t)^{12}}{3628800};$$

$$N = 8, \qquad \rho^2 = 1 - \frac{(\omega \Delta t)^8}{40320} + \frac{(\omega \Delta t)^{10}}{134400} - \frac{(\omega \Delta t)^{12}}{2903040} + \frac{(\omega \Delta t)^{14}}{203212800};$$

$$N = 9, \qquad \rho^2 = 1 - \frac{(\omega \Delta t)^{10}}{453600} + \frac{(\omega \Delta t)^{12}}{4354560} - \frac{(\omega \Delta t)^{14}}{152409600} + \frac{(\omega \Delta t)^{16}}{14631321600}. \qquad (28)$$

From equations (27) and (28) one concludes:

The spectral radius can be larger than one for $N = 2, 3, 6, 7$, for a small value of $\omega \Delta t$. This is because in this case, the term immediately following 1 is the dominant one, and is positive.

The spectral radius is less than one for a finite value of $\omega \Delta t$ for $N = 4, 5, 8, 9$, etc., because the term immediately following 1 is the dominant one and it is negative.

In practice, using ten digit calculations, one can observe that for $N > 3$, the spectral radius defined by equation (25) is equal to one for a limited range of $\omega \Delta t$. Table 1 shows those ranges. This table has been obtained using the MAPLE V package. In some cases, there exists two or more of these ranges. In fact, the spectral radius is a little larger than one between those ranges, as shown in Table 2.

The spectral radius is plotted as a function of $\omega \Delta t$ for even and odd values of N in Figures 3 and 4, respectively. Remember that the central difference scheme is stable for $\omega \Delta t \leqslant 2$ [17]. The critical time segment length increases with the order N. For $N = 29$, the critical time segment is five times the critical time step corresponding to the central difference scheme.

From stability analysis, one concludes that DAM is conditionally stable, and thus the time segment will be a function of the smallest period of vibration of the discrete problem. This is similar to the central difference scheme. To overcome this limitation, one can apply DAM in the modal space using the appropriate number of modes. Some numerical results combining mode superposition and DAM will be presented. In order to demonstrate and prove the validity of the present work, some particular cases are discussed in the following sections.

TABLE 1

$\omega\Delta t$ ranges for which the spectral radius in less than one

Order N	$\rho([\mathbf{A}]) \leqslant 1$	Order N	$\rho([\mathbf{A}]) \leqslant 1$
2	$\omega\Delta t = 0$	3	$\omega\Delta t = 0$
4	$0 < \omega\Delta t < 2{\cdot}17$	5	$0 < \omega\Delta t < 2{\cdot}65$
6	$0 < \omega\Delta t < 0{\cdot}8,\ 2{\cdot}2 < \omega\Delta t < 3{\cdot}17$	7	$0 < \omega\Delta t < 0{\cdot}24$
8	$0 < \omega\Delta t < 2{\cdot}00$	9	$0 < \omega\Delta t < 3{\cdot}08$
10	$0 < \omega\Delta t < 0{\cdot}5,\ 2{\cdot}00 < \omega\Delta t < 4{\cdot}68$	11	$0 < \omega\Delta t < 0{\cdot}87,\ 3{\cdot}79 < \omega\Delta t < 5{\cdot}14$
12	$0 < \omega\Delta t < 1{\cdot}8,\ 5{\cdot}59 < \omega\Delta t < 5{\cdot}92$	13	$0 < \omega\Delta t < 3{\cdot}62$
14	$0 < \omega\Delta t < 1{\cdot}5,\ 1{\cdot}8 < \omega\Delta t < 5{\cdot}4$	15	$0 < \omega\Delta t < 1{\cdot}6,\ 3{\cdot}60 < \omega\Delta t < 6{\cdot}02$
16	$0 < \omega\Delta t < 2{\cdot}15,\ 5{\cdot}3 < \omega\Delta t < 6{\cdot}28$	17	$0 < \omega\Delta t < 3{\cdot}44$
18	$0 < \omega\Delta t < 5{\cdot}2$	19	$0 < \omega\Delta t < 2{\cdot}8,\ 3{\cdot}5 < \omega\Delta t < 6{\cdot}92$
20	$0 < \omega\Delta t < 3{\cdot}3,\ 5{\cdot}2 < \omega\Delta t < 8{\cdot}3$	21	$0 < \omega\Delta t < 3{\cdot}6,\ 6{\cdot}93 < \omega\Delta t < 8{\cdot}80$
22	$0 < \omega\Delta t < 5{\cdot}2,\ 8{\cdot}6 < \omega\Delta t < 9{\cdot}47$	23	$0 < \omega\Delta t < 6{\cdot}9$
24	$0 < \omega\Delta t < 4{\cdot}5,\ 5{\cdot}2 < \omega\Delta t < 8{\cdot}40$	25	$0 < \omega\Delta t < 4{\cdot}5,\ 6{\cdot}8 < \omega\Delta t < 9{\cdot}33$
26	$0 < \omega\Delta t < 2{\cdot}46,\ 3{\cdot}80 < \omega\Delta t < 4{\cdot}9$ $8{\cdot}5 < \omega\Delta t < 10{\cdot}73$	27	$0 < \omega\Delta t < 6{\cdot}9,\quad 10{\cdot}12 < \omega\Delta t < 11{\cdot}07$
28	$0 < \omega\Delta t < 2{\cdot}00,\ 2{\cdot}50 < \omega\Delta t < 8{\cdot}63$	29	$0 < \omega\Delta t < 6{\cdot}00,\ 6{\cdot}8 < \omega\Delta t < 10{\cdot}06$

4. APPLICATIONS TO SINGLE-DEGREE-OF-FREEDOM PROBLEMS

4.1. FREE VIBRATION

In this section, a proof of convergence for the free vibration of a single-degree-of-freedom system subjected to initial conditions is presented. Two cases are considered: with damping ($c \neq 0$) and without damping ($c = 0$). For the damping case, numerical results are presented for values of the damping ratio that result in overdamped, critically damped, and underdamped solutions [16].

TABLE 2

Spectral radii for different values of $\omega\Delta t$ for $N = 21$ and $N = 29$

N			
21		29	
$\omega\Delta t$	ρ	$\omega\Delta t$	ρ
1	1·000000000	1	1·000000000
3·6	1·000000000	5	1·000000000
3·7	1·000000002	5·9	1·000000001
4	1·000000020	6·5	1·000000004
5	1·000004626	6·7	1·000000001
6	1·000157417	6·8	0·9999999943
6·6	1·000423213	7	0·9999999535
6·8	1·000253131	8	0·9999918278
7	0·9994574529	9	0·9997734248
8	0·9193617507	10	0·9996019758
8·5	0·5946234109	10·1	1·000181899
8·79	0·9907726421	11	1·066867469
9	1·158566290	12	1·791713875

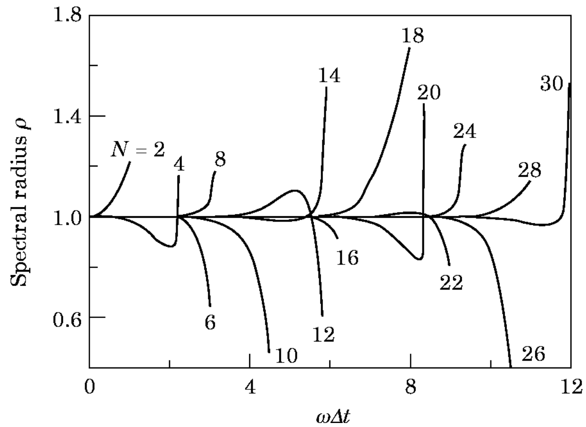

Figure 3. Spectral radius in function of $\omega\Delta t$ for N even.

4.1.1. *Proof of convergence*

The ordinary differential SDOF free vibration equation of a discrete spring–damper–mass system with initial conditions can be written as

$$\mathrm{d}^2u/\mathrm{d}t^2 + 2\xi\omega\,\mathrm{d}u/\mathrm{d}t + \omega^2 u = 0, \qquad \omega^2 = k/m, \qquad 2\xi\omega = c/m,$$
$$u(t=0) = u_0, \qquad \mathrm{d}u(t=0)/\mathrm{d}t = u_1, \tag{29}$$

where u is the displacement, k the stiffness of the spring, c the damping coefficient and m the mass supported by the spring. The analytical solution of the differential equation (29) in the case of undamped vibrations ($c = 0$) is

$$u(t) = u_0 \cos(\omega t) + (u_1/\omega)\sin(\omega t). \tag{30a}$$

Using power series expansions of sine and cosine functions, equation (30a) is written:

$$u(t) = u_0\left(1 - \frac{(\omega t)^2}{2!} + \frac{(\omega t)^4}{4!} - \frac{(\omega t)^6}{6!} + - \cdots\right) + \frac{u_1}{\omega}\left(\frac{(\omega t)}{1!} - \frac{(\omega t)^3}{3!} + \frac{(\omega t)^5}{5!} - \; + \cdots\right), \tag{30b}$$

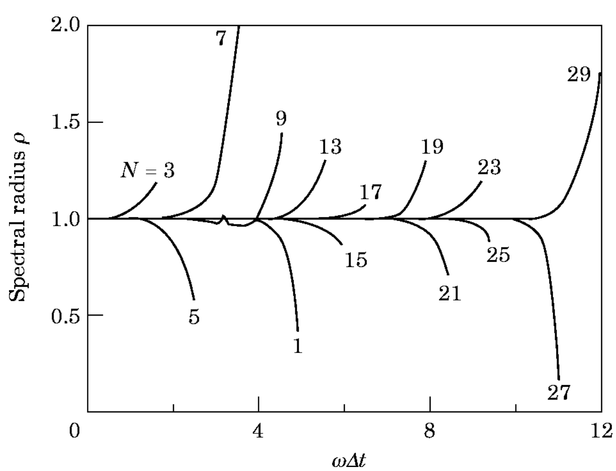

Figure 4. Spectral radius in function of $\omega\Delta t$ for N odd.

$$u(t) = \left(u_0 + \frac{u_1}{\omega}\frac{(\omega t)}{1!} - u_0\frac{(\omega t)^2}{2!} - \frac{u_1}{\omega}\frac{(\omega t)^3}{3!} + u_0\frac{(\omega t)^4}{4!} + \frac{u_1}{\omega}\frac{(\omega t)^5}{5!} - u_0\frac{(\omega t)^6}{6!} - + \cdots \right). \tag{30c}$$

Using the asymptotic expansion defined in equation (4) and the recursive solution of equation (9), the following solution is obtained:

$$u_2 = \frac{-1}{2m}[ku_0] = \frac{-1}{2}[\omega^2 u_0]; \qquad u_3 = \frac{-1}{6}[\omega^2 u_1] = \frac{-u_1}{3!\omega}\omega^3; \qquad u_4 = \frac{-1}{4\times 3}[\omega^2 u_2] = \frac{u_0}{4!}\omega^4,$$

$$u_5 = \frac{-1}{5\times 4}[\omega^2 u_3] = \frac{u_1}{5!\omega}\omega^5, \qquad u_6 = \frac{-1}{6\times 5}[\omega^2 u_4] = \frac{-u_0}{6!}\omega^6, \ldots . \tag{31}$$

It is seen from equation (31) that the asymtotic equation converges to the analytical solution (30) if an infinite asymptotic expansion of the solution $u(t)$ is adopted. This demonstrates the convergence of the asymptotic expansion. When damping is present, the analytical solution of the differential equation (29) becomes

$$u(t) = e^{-\xi\omega t}\left[u_0 \cos(\omega_D\, t) + \left(\frac{u_1 + \xi\omega u_0}{\omega_D}\right)\sin(\omega_D\, t)\right], \qquad \omega_D = \omega\sqrt{1-\xi^2}. \tag{32a}$$

Using the expansions of the sine, cosine, and exponential functions, equation (32a) can be written:

$$\begin{aligned} u(t) = \Bigg[& u_0\left(1 - \frac{(\omega_D\, t)^2}{2!} + \frac{(\omega_D\, t)^4}{4!} - \frac{(\omega_D\, t)^6}{6!} + \ - \cdots\right) \\ & + \frac{u_1 + \xi\omega u_0}{\omega_D}\left(\frac{(\omega_D\, t)}{1!} - \frac{(\omega_D\, t)^3}{3!} + \frac{(\omega_D\, t)^5}{5!} - + \cdots\right)\Bigg] \\ & \times \left[1 - \omega\xi t + \frac{(\omega\xi t)^2}{2!} - \frac{(\omega\xi t)^3}{3!} + \frac{(\omega\xi t)^4}{4!} - \frac{(\omega\xi t)^5}{5!} + - \cdots\right], \end{aligned} \tag{32b}$$

$$\begin{aligned} u(t) = {} & u_0 + tu_1 - \frac{t^2}{2!}[2\omega\xi u_1 + (\omega^2\xi^2 + \omega_D^2)u_0] \\ & + \frac{t^3}{3!}[(-\omega_D^2 + 3\omega^2\xi^2)u_1 + (\omega^2\xi^2 + 2\omega_D^2\,\xi\omega + 2\omega^3\xi^3)u_0] - \ + \cdots . \end{aligned} \tag{32c}$$

With the definition of the damped natural frequency ω_D equation (32c) can be written as

$$u(t) = u_0 + tu_1 - \frac{t^2}{2!}[2\omega\xi u_1 + \omega^2 u_0] + \frac{t^3}{3!}[(1+4\xi^2)\omega^2 u_1 + 2\xi\omega^3 u_0] - + \cdots . \tag{33}$$

Using the asymptotic expansion given in equation (4) and the recursive solution of equation (9), the following solution is obtained:

$$u_2 = (-1/2m)[cu_1 + ku_0] = (-1/2)[2\xi\omega u_1 + \omega^2 u_0];$$

$$u_3 = (-1/6)[4\xi\omega u_2 + \omega^2 u_1] = (1/6)[(1+4\xi^2)\omega^2 u_1 + 2\xi\omega^3 u_0], \cdots . \tag{34}$$

Once again, it is observed, that the asymptotic method converges to the analytical solution when an infinite expansion is considered.

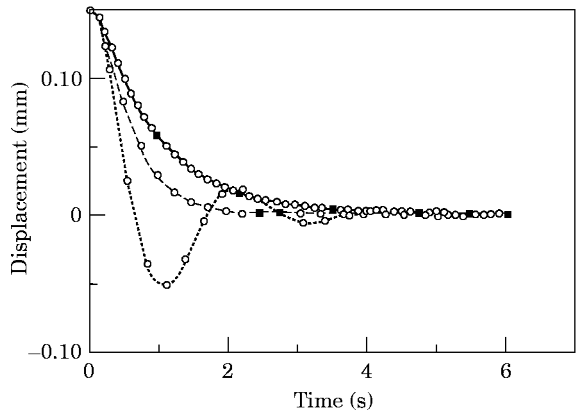

Figure 5. SDOF, damped free vibration example: ——, overdamping exact solution; ····, underdamping exact solution; - - - -, critical damping exact solution; ○, DAM intermediate values; ■, DAM time segment change.

4.1.2. *Numerical examples*

To illustrate the application of DAM, the solution of the free vibration damping problem (equation 29) using an asymptotic development using 30 terms in the series ($N = 30$) is presented. The parameter ε (equation 18) to compute the critical time has been set to 10^{-6}. The data for this problem are $k = 10$ and $m = 1$ and the initial conditions are $u_0 = 0{\cdot}15$ and $u_1 = 0$. The analytical solutions [15, 16] for three damping values are given as:

$$u(t) = -0{\cdot}0218\, e^{-8.873t} + 0{\cdot}1718\, e^{-1{\cdot}127t}, \qquad \text{for the overdamped case } (c = 10);$$

$$u(t) = (0{\cdot}15 + 0{\cdot}4743t)\, e^{-3{\cdot}1623t}, \qquad \text{for the critically damped case } (c = \sqrt{40});$$

$$u(t) = e^{-t}(0{\cdot}15 \cos(3t) + 0{\cdot}05 \sin(3t)), \qquad \text{for the underdamped case } (c = 2).$$

In Figure 5, the results obtained with the dynamic asymptotic method using a series of order 30 are compared to the analytical results for $0 < t < 6$. The critical time computed with equation (18) is marked by a black box on the curves. Between two values of the critical time, some intermediate values computed with the polynomial series are also shown. Therefore, it is observed that in order to obtain a solution between time $t = 0$ and $t = 4{\cdot}0$, only four time segments are needed with DAM for the overdamped case ($t_{crit} = 0{\cdot}96$, $2{\cdot}13$, $3{\cdot}45$ and $4{\cdot}75$). For the underdamped ($t_{crit} = 2{\cdot}71$ and $6{\cdot}04$) and critically damped cases ($t_{crit} = 2{\cdot}40$ and $5{\cdot}48$), only two segments are required. For a lower order of the series, more time segments would be necessary to obtain accurate results. For explicit or implicit schemes, the number of time steps required for convergence is larger than 3. It is seen that the DAM results are in good agreement with the analytical solution, and the solution is obtained with fewer time segments than with explicit or implicit integration schemes.

One can observe, from the stability analysis (section 3), that the critical value of $\omega\Delta t$ is equal to $11{\cdot}7$ for $N = 30$ which gives $\Delta t = 3{\cdot}9$. Since the actual value t_{crit} is smaller than Δt, one concludes that the criterion used to achieve an accurate solution (equation 18) is thus more restrictive than the stability criterion. The results for a MDOF problem obtained from the Newmark-β scheme are compared with the DAM in the next section.

4.2. UNDAMPED FORCED VIBRATION

In this section, a proof of convergence is given for two transient vibration problems. Numerical results are presented for the case of harmonic loading in the form of a cosine series for three exciting frequencies (Ω): standard vibration ($\Omega \neq \omega$), resonance ($\Omega = \omega$) and vibration with beat phenomenon ($\Omega \approx \omega$).

4.2.1. *Proof of convergence for constant and harmonic load cases*

It is proved in this section that the DAM also converges to the analytical solution for two types of loading:

$$f(t) = \mathrm{d}^2u/\mathrm{d}t^2 + \omega^2 u, \qquad \text{with } f = F_1/m \text{ for constant load}$$
$$\text{and} \qquad f(t) = (F_2/m)\cos(\Omega t) \text{ for harmonic load.} \tag{35}$$

The analytical solution for the constant load is given by

$$u(t) = (u_0 - F_1/k)\cos(\omega t) + \frac{u_1}{\omega}\sin\omega t + F_1/k. \tag{36}$$

Using the asymptotic expansion defined in equation (4) and the recursive solution of equation (9), the following solution is obtained:

$$u_2 = \frac{-\omega^2}{2!}\left[u_0 - \frac{F_1}{k}\right], \qquad u_3 = \frac{-u_1}{3!\omega}\omega^3, \qquad u_4 = \frac{\omega^4}{4!}\left[u_0 - \frac{F_1}{k}\right],$$
$$u_5 = \frac{u_1}{5!\omega}\omega^5, \qquad u_6 = \frac{-\omega^6}{6!}\left[u_0 - \frac{F_1}{k}\right], \ldots. \tag{37}$$

The polynomial series expansion of equation (36) is similar to the one defined by equation (30c) except that u_0 is replaced by $(u_0 - F_1/k)$. Therefore, it is again seen that DAM converges to the exact solution if an infinite series is used. It can also be demonstrated that the same conclusion can be drawn if damping is included.

For the harmonic forced vibration with a cosine function, the analytical solution is given by the following equation when $u_0 = u_1 = 0$ if $\Omega \neq \omega$:

$$u(t) = \frac{F_2}{k}\left(\frac{\omega^2}{[\omega^2 - \Omega^2]}\right)(\cos(\Omega t) - \cos(\omega t)). \tag{38a}$$

The polynomial series of equation (38a) is given by:

$$\cos(\Omega t) - \cos(\omega t) = -2(\sin(\Omega - \omega)t/2)(\sin(\Omega + \omega)t/2),$$
$$u(t) = \frac{\omega^2 F_2}{k}\left(\frac{t^2}{2!} - \frac{(\omega^2 + \Omega^2)t^4}{4!} + \frac{(\Omega^4 + \Omega^2\omega^2 + \omega^4)t^6}{6!} - + \cdots\right). \tag{38b}$$

To use the DAM given by equation (9), the cosine loading function must be developed in a polynomial series as

$$f(t) = (F_2/m)(1 - (\Omega t)^2/2! + (\Omega t)^4/4! - (\Omega t)^6/6! + - \cdots). \tag{39}$$

Using equation (39) with equation (9), the solution can be written as

$$u_2 = \frac{\omega^2}{2!}\frac{F_2}{k}, \qquad u_3 = 0, \qquad u_4 = \frac{-\omega^2}{4!}\frac{F_2}{k}(\Omega^2 + \omega^2), \qquad u_5 = 0, \tag{40}$$

$$u_6 = \frac{\omega^2}{6!}\frac{F_2}{k}(\Omega^4 + \Omega^2\omega^2 + \omega^4), \ldots .$$

For this particular harmonic load, the DAM results converge to the analytical solution when N becomes infinity. The same conclusion can be drawn for the damped case with a sinusoidal loading function. In the case of resonance which corresponds to $\Omega = \omega$, the solution from the DAM is as follows:

$$u(t) = (F_2/k)(\omega t/2)[(\omega t) - (\omega t)^3/3! + (\omega t)^5/5! - (\omega t)^7/7! + - \cdots], \tag{41}$$

When N reaches infinity,

$$u(t) = (F_2/k)(\omega t/2)\sin(\omega t) = (F_2/2\omega m)t \sin(\omega t). \tag{42}$$

Equation (39) is the resonant response of an undamped system [16].

4.2.2. *Numerical examples*

To validate the application of the present method for transient dynamics problems, solutions are presented for an undamped system ($c = 0$) subjected to a cosine load with initial displacement and velocity set to 0 ($u_0 = u_1 = 0$). The frequency ratios Ω/ω are 0·5, 0·9 and 1 and the other input data are $k = m = F_2 = 1$.

In Figures 6–8, the analytical results are compared with those obtained from the DAM for a value of the order N of 30 (order 28 for the load) for $\Omega/\omega = 0{\cdot}5$, 0·9 and 1, respectively. The critical times calculated from equation (18) are marked with black boxes and intermediate values obtained with the time polynomial series are also shown. Table 3 gives the critical times and time segment lengths for $0 < t < 90$. The time segment lengths computed with equation (18) are approximately 9·3 for the three cases. Using results of section 3, the critical value of $\omega\Delta t$ is 11·7 for $N = 30$ which gives $\Delta t = 11{\cdot}7$ ($\omega = 1$). This example, compared to the previous one (see Figure 5), confirms that the time segment

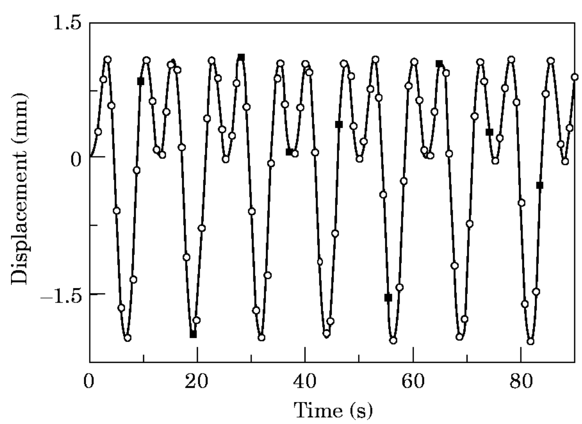

Figure 6. SDOF, harmonic load, $\Omega/\omega = 0{\cdot}5$: ——, analytical solution; ○, DAM intermediate values; ■, DAM time segment change.

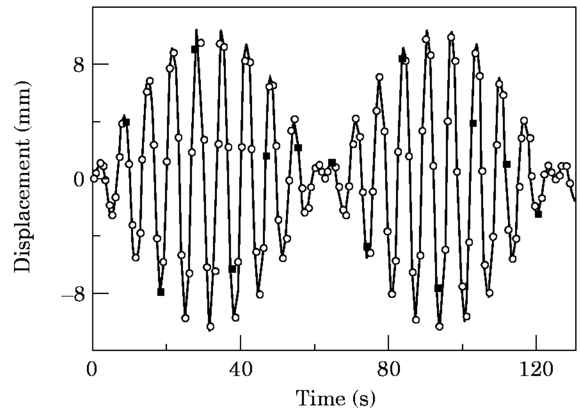

Figure 7. SDOF, harmonic load, $\Omega/\omega = 0{\cdot}9$: ——, analytical solution; ○, DAM intermediate values; ■, DAM time segment change.

length is a function of the frequency ω. Once again, equation (18) gives a smaller time segment length than the one computed from stability considerations.

For these three cases, it is noted that the number of time segments per period of vibration is between 1 and 2. For an implicit method, more time steps are needed. Using the criterion proposed by Bathe and Wilson [14] to compute the time step (smallest period divided by ten), 20 time steps per period (approximately 140 steps for $t = 0$ to $t = 90$) are required. In order to accurately predict the maximum displacement shown in Figure 6, four time segments per period of oscillation are necessary.

It is noted in Figure 7 that the beat phenomenon is well represented without any modification in the algorithm and the resonance phenomenon is also clearly seen in Figure 8.

5. APPLICATIONS TO MULTI DEGREE-OF-FREEDOM PROBLEMS

Two examples are presented here to validate DAM and MDAM for multi-degree-of-freedom problems. The first example is to demonstrate the versatility of the DAM and

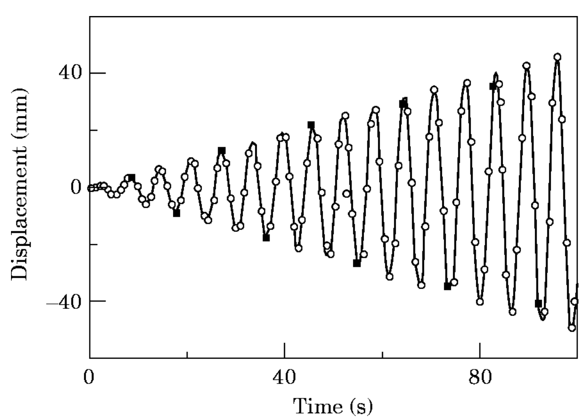

Figure 8. SDOF, harmonic load, $\Omega/\omega = 1{\cdot}0$: ——, analytical solution; ○, DAM intermediate values; ■, DAM time segment change.

TABLE 3

Critical time segments for SDOF with cosine load with different frequency excitations

Ω/ω = 0·5 Critical time	Time segment	Ω/ω = 0·9 Critical time	Time segment	Ω/ω = 1 Critical time	Time segment
9·21	9·21	8·78	8·78	8·45	8·45
18·50	9·29	18·07	9·29	17·40	8·95
27·88	9·38	27·58	9·51	26·65	9·25
37·21	9·33	37·10	9·52	35·97	9·32
46·40	9·19	46·51	9·41	45·32	9·35
55·67	9·27	55·58	9·07	54·68	9·36
65·07	9·40	64·59	9·01	64·04	9·36
74·43	9·36	73·88	9·29	73·40	9·36
83·57	9·14	83·89	10·01	82·77	9·37
92·68	9·11	93·45	9·56	92·14	9·37
Mean value	9·27	Mean value	9·34	Mean value	9·21

to compare the results to those obtained with the Newmark-β integration scheme. The influence of varying the value of the parameter ε defined in equation (18) will also be demonstrated. The second example deals with 40 degrees of freedom and mode superposition is used. DAM will be applied to each uncoupled equation. The influence of varying the order N on computing time will be analyzed.

5.1. THREE-DEGREE-OF-FREEDOM EXAMPLE

A simple 2D frame idealized using three DOF is shown in Figure 9. Two types of loads are considered: a constant load and a cosine load. In both cases, the order of the series is 30 and ε is set to 10^{-6}. The mass and rigidity matrices are

$$[\mathbf{M}] = \begin{bmatrix} 0{\cdot}175 & 0 & 0 \\ 0 & 0{\cdot}263 & 0 \\ 0 & 0 & 0{\cdot}350 \end{bmatrix} \text{kNs}^2/\text{mm}, \qquad [\mathbf{K}] = 105 \begin{bmatrix} 1 & -1 & 0 \\ -1 & 3 & -2 \\ 0 & -2 & 5 \end{bmatrix} \text{kN/mm}.$$

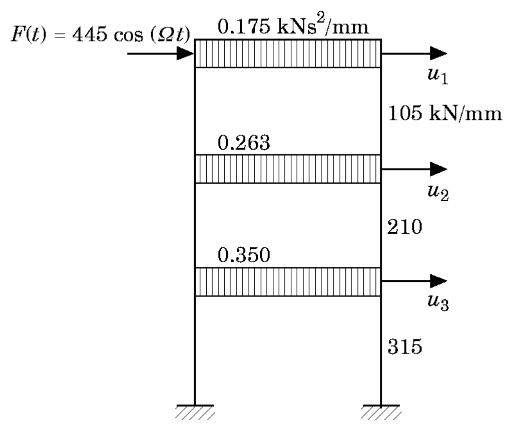

Figure 9. Three-degrees-of-freedom example.

5.1.1. *Forced vibration with a constant load*

The analytical solution is given by [18]

$$\begin{Bmatrix} u_1(t) \\ u_2(t) \\ u_3(t) \end{Bmatrix} = \begin{bmatrix} 1{\cdot}0 & 1{\cdot}0 & 1{\cdot}0 \\ 0{\cdot}644 & -0{\cdot}601 & -2{\cdot}570 \\ 0{\cdot}300 & -0{\cdot}676 & 2{\cdot}470 \end{bmatrix} \begin{Bmatrix} 6{\cdot}719(1-\cos(14{\cdot}5t)) \\ 1{\cdot}070(1-\cos(31{\cdot}1t)) \\ 0{\cdot}052(1-\cos(46{\cdot}1t)) \end{Bmatrix}.$$

In Figure 10, the analytical response and the response obtained with the DAM are shown. The critical time segments are marked with black boxes and intermediate values obtained with the time polynomial series are also shown (empty circles). Table 4 gives the critical time values and time segment lengths for $0 < t < 2$ s. It can be seen that the results obtained with the DAM are exact. Two time segments per period of vibration (the largest period of vibration is 0·43 s) are necessary to converge to the exact solution. The time segment lengths obtained with equation (18) is equal to 0·2 s. From a stability point of view, the critical time segment length, computed using $\omega = 46{\cdot}1$ rad/s, is equal to 0·25 s. Thus, equation (18) with $\varepsilon = 10^{-6}$ gives smaller time segment lengths than the ones obtained from stability considerations.

In Figure 11, the numerical response obtained with the Newmark-β method using two different time step values ($\Delta t = 0{\cdot}01$ and 0·05 s) are compared to the response obtained from the DAM. The number of time steps to obtain the solution between $t = 0$ and $t = 2$ s are 200 and 40, respectively. With the DAM, ten time segments are necessary to obtain the exact solution. It is noted that the convergence is poor with $\Delta t = 0{\cdot}05$ s whereas the one obtained with $\Delta t = 0{\cdot}01$ s is relatively good.

It is concluded that the results obtained with the DAM are better than those obtained with the implicit scheme for the following reasons: (1) the response with the DAM is practically exact; (2) one needs only ten time segments to find the response compared to 40 and 200 time steps for the Newmark-β method with $\Delta t = 0{\cdot}01$ s and 0·05 s, respectively; (3) no aliasing phenomenon appears with the DAM; (4) the time segment is automatically estimated by the algorithm.

5.1.2. *Forced vibration with harmonic load*

The same structure has been studied with a cosine loading function using two frequency ratios: $\Omega/\omega_1 = 0{\cdot}9$ and 1·0. Table 4 gives critical time values and time segment lengths for $0 < t < 4$ s. In Figures 12 and 13, the response obtained with the DAM and the one obtained with the Newmark-β algorithm, using two time step values ($\Delta t = 0{\cdot}01$ s and 0·05 s) are shown. As in the previous loading case, the convergence with $\Delta t = 0{\cdot}05$ s is poor, and the one obtained with $\Delta t = 0{\cdot}01$ s is relatively good. To obtain the response between $t = 0$ and $t = 4$ s, 400 time steps are needed for $\Delta t = 0{\cdot}01$ s and 80 for $\Delta t = 0{\cdot}05$ s. The DAM converges to the exact solution with only 20 time segments.

5.1.3. *Effect of the convergence tolerance* ε

Using equation (18), it is possible to find critical time values for which the error between two consecutive orders of asymptotic development is less than ε. But this critical time or the time segment length does not guarantee that the solution will be stable. To show the effect of the convergence criterion, the same problem is solved using a constant load and varying the value of $\varepsilon(\varepsilon = 10^{-2}, 10^{-3}, 10^{-4}$ and $10^{-5})$. Results for $\varepsilon = 10^{-2}$, 10^{-3} and the exact solution are shown in Figure 14. For values of ε varying from 10^{-4} to 10^{-5}, solutions obtained with the DAM and the exact solution are perfectly superposed. For $\varepsilon = 10^{-2}$, one observes that the solution is unstable, and for $\varepsilon = 10^{-3}$, the solution is less accurate than

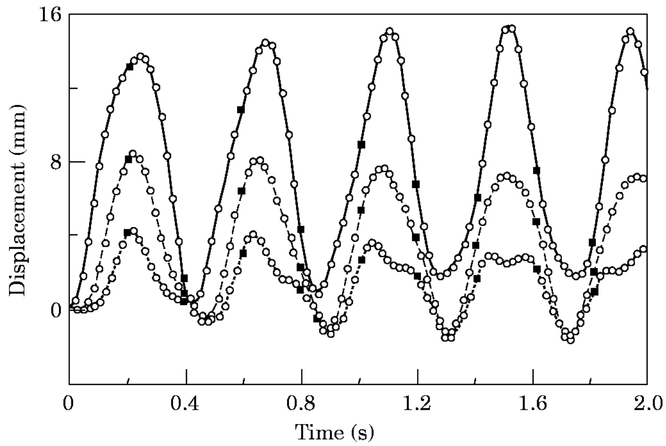

Figure 10. Three DOF response for constant load, $\Omega/\omega_1 = 0$: ——, analytical solution: u_1; - - - -, analytical solution: u_2; ····, analytical solution: u_3; ○, DAM intermediate values; ■, DAM time segment change.

the one obtained with $\varepsilon = 10^{-5}$. The minimum and maximum values of time segment lengths are shown in Table 5.

From stability considerations, the critical time segment length has been found previously to equal 0·25 s. Therefore, the solution is unstable with $\varepsilon = 10^{-2}$ since, for this value of

TABLE 4

Critical time segments for three DOF problem with cosine load with different frequency excitations

Ω/ω					
0·0		1·0		0·9	
Critical time	Time segment	Critical time	Time segment	Critical time	Time segment
0·19	0·19	0·20	0·20	0·20	0·20
0·39	0·20	0·39	0·19	0·39	0·19
0·58	0·19	0·59	0·20	0·59	0·20
0·79	0·21	0·80	0·21	0·80	0·21
1·00	0·21	1·00	0·20	1·00	0·20
1·19	0·19	1·21	0·21	1·21	0·21
1·40	0·21	1·42	0·21	1·42	0·21
1·61	0·21	1·63	0·21	1·62	0·20
1·81	0·20	1·84	0·21	1·82	0·20
2·03	0·22	2·04	0·20	2·02	0·20
–	–	2·25	0·22	2·23	0·21
–	–	2·46	0·21	2·44	0·21
–	–	2·68	0·22	2·64	0·20
–	–	2·89	0·21	2·85	0·21
–	–	3·11	0·22	3·06	0·21
–	–	3·33	0·22	3·26	0·20
–	–	3·54	0·21	3·47	0·21
–	–	3·76	0·22	3·67	0·20
–	–	3·97	0·21	3·86	0·19
–	–	4·19	0·22	4·06	0·20
Mean value	0·20	Mean value	0·21	Mean value	0·20

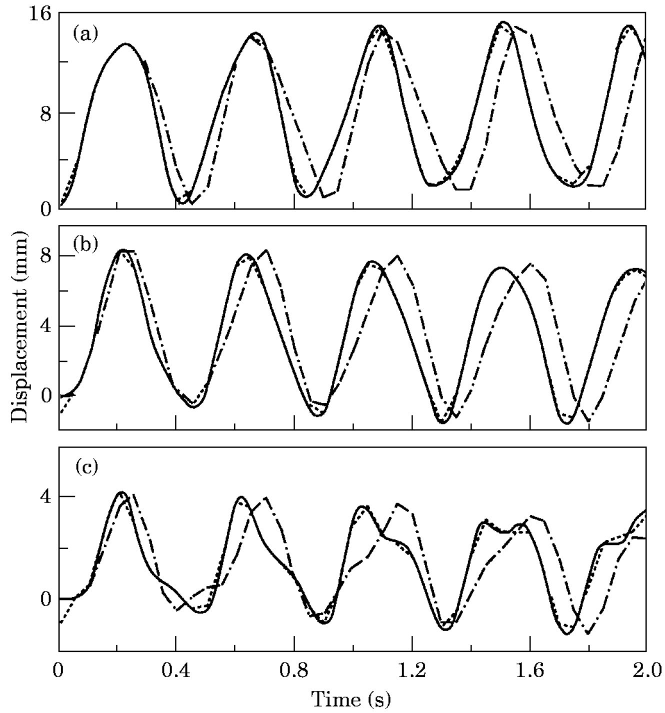

Figure 11. Three DOF response for constant load, $\Omega/\omega_1 = 0$: ——, DAM; ····, Newmark $\Delta t = 0{\cdot}01$; –·–·, Newmark $\Delta t = 0{\cdot}05$; (a) displacement u_1; (b) displacement u_2; (c) displacement u_3.

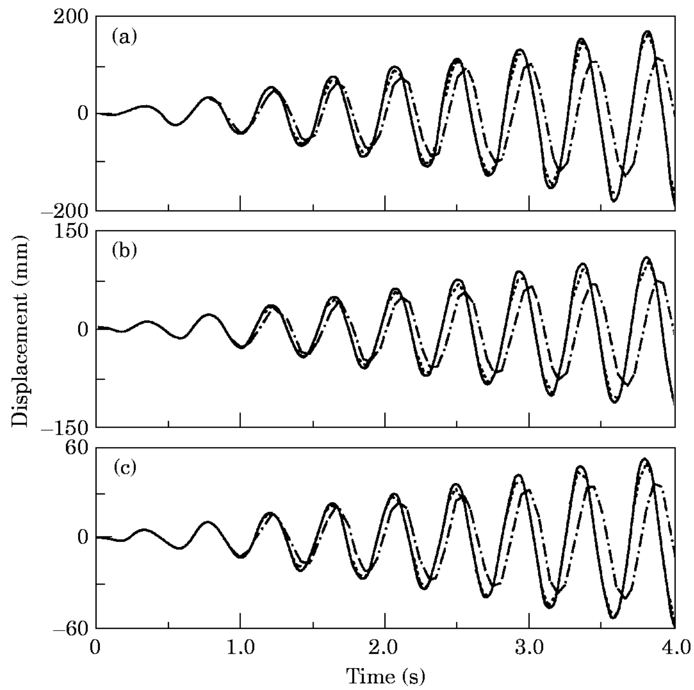

Figure 12. Three DOF response for harmonic load, $\Omega/\omega_1 = 1{\cdot}0$: ——, DAM; ····, Newmark $\Delta t = 0{\cdot}01$; –·–·, Newmark $\Delta t = 0{\cdot}05$; (a) displacement u_1; (b) displacement u_2; (c) displacement u_3.

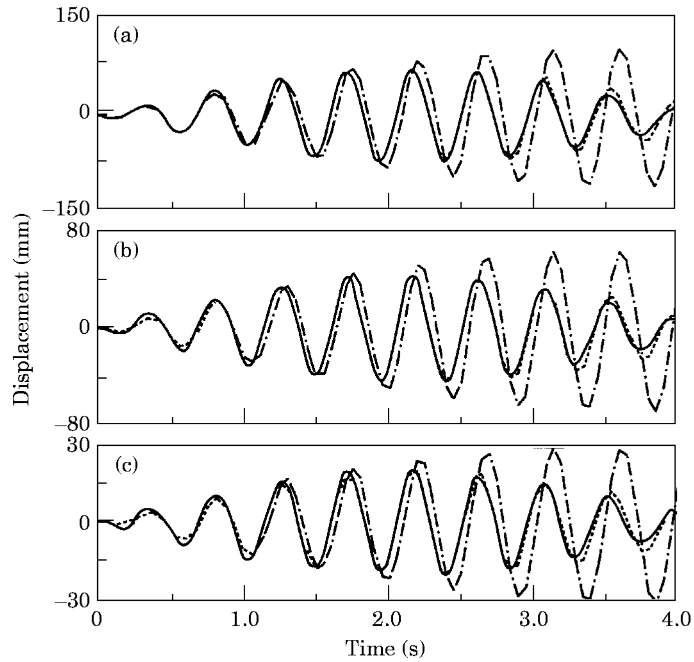

Figure 13. Three DOF response for harmonic load, $\Omega/\omega_1 = 0{\cdot}9$: ——, DAM; ····, Newmark $\Delta t = 0{\cdot}01$; –·–·, Newmark $\Delta t = 0{\cdot}05$; (a) displacement u_1; (b) displacement u_2; (c) displacement u_3.

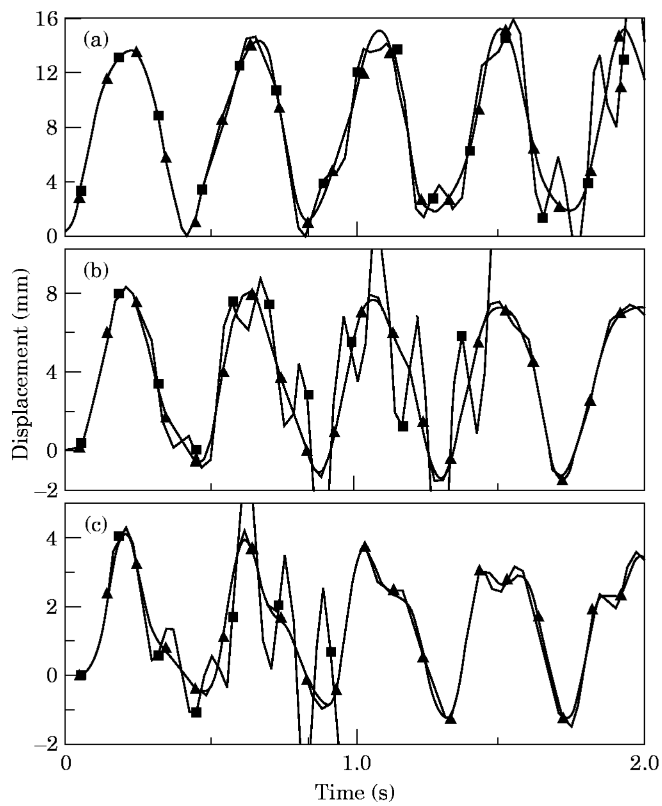

Figure 14. Three DOF response for constant load, $\Omega/\omega_1 = 0{\cdot}0$: ——, analytical solution; –■–, DAM with $\varepsilon = 10^{-2}$; –▲–, DAM with $\varepsilon = 10^{-3}$; (a) displacement u_1; (b) displacement u_2; (c) displacement u_3.

TABLE 5

Time segment lengths for different values of ε

ε	Minimum	Maximum	Mean value
10^{-2}	0·25402	0·27175	0·25661
10^{-3}	0·23342	0·24953	0·24364
10^{-4}	0·21941	0·24689	0·22762
10^{-5}	0·20713	0·22094	0·21057
10^{-6}	0·19111	0·22335	0·20189

TABLE 6

Beam under constant load: *period values*

Mode number	1	2	3	4
Period (s)	2.84×10^{-4}	3.02×10^{-4}	8.86×10^{-4}	3.54×10^{-3}

ε, the time segment length is always larger than 0·25 s. For the other case, the time segment length is less than 0·25 s and thus, solutions are stable.

5.2. EXAMPLE WITH FORTY DEGREES OF FREEDOM

For the last application, the solution of the multi-degree-of-freedom problem shown in Figure 15 [19] is presented. The time–displacement response is shown in Figure 16. One uses the DAM coupled with a mode superposition technique, retaining the four first modes. The corresponding periods are given in Table 6.

The objective of this problem, is to show the effect of the order N of asymptotic development on the CPU time requirements. The order of N is varied from 10 to 100.

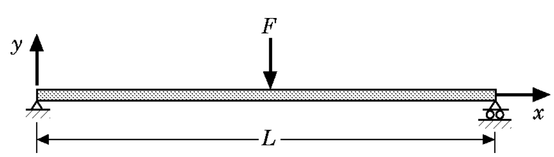

Figure 15. Simply supported beam loaded by a constant load with: $L = 1{\cdot}19$ m; $\rho = 2{\cdot}96 \times 10^3$ kg/m^3; $A = 0{\cdot}51 \times 10^{-2}$ m^2; $I = 0{\cdot}944 \times 10^{-5}$ m^4; $E = 10{\cdot}48 \times 10^{10}$ N/m^2; $F = 4{\cdot}448$ N.

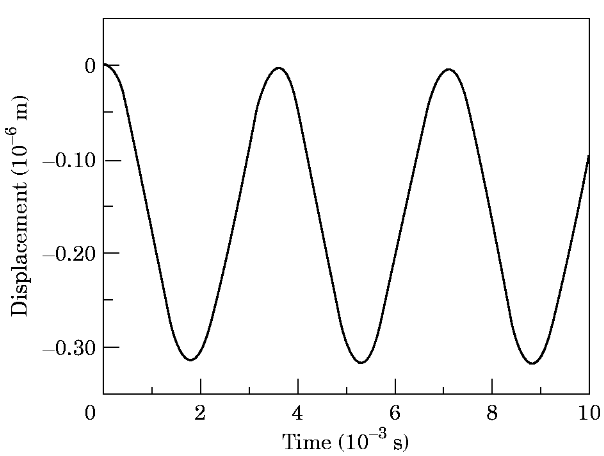

Figure 16. Dynamic response of the simply supported beam subjected to a constant load.

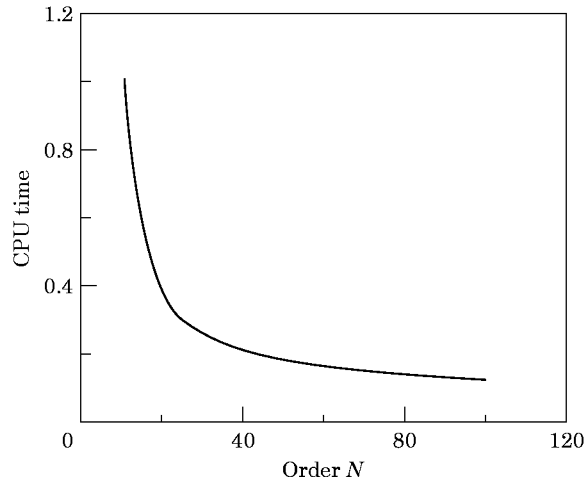

Figure 17. Relative CPU time for different values of N.

Figure 17 shows the relative CPU time, excluding eigenvalue calculations, as a function of N. Equation (18c) has been used to compute the critical time segment length with $\varepsilon = 10^{-6}$. For every order, the same solution was obtained.

One can conclude from Figure 17, that the higher the order, the shorter is the CPU time required to get the solution. However, for an order N larger than 50, negligible reductions in CPU time are obtained.

6. CONCLUSION

A novel approach, called the Dynamic Asymptotic Method (DAM), has been presented. This method can effectively be used for the solution of linear transient dynamics problems. The method is similar to the analytical method undetermined coefficients and power series methods used to find the analytical solution of ordinary differential equations. It has been demonstrated that the DAM results converge to the analytical solution when the maximum power of the polynomial series reaches infinity. The DAM can be considered as a semi-analytical method.

In practical problems, the maximum power of the series must be limited. Therefore, there is a limit, called t_{crit}, beyond which the series diverges. In the present work, a method has been proposed to compute the value of t_{crit} automatically during the solution procedure. Stability results have also been presented as a function of N. From examples presented in this paper one can observe that the critical time segment lengths evaluated with equation (18) is smaller than the one estimated from stability considerations if ε is less than 10^{-3}. A good compromise is $\varepsilon = 10^{-4}$. The solution obtained with the DAM is continuous for any time value. At the critical time, the displacements and their first derivatives (velocities) are continuous.

It is concluded that the proposed DAM is more efficient than the standard integration techniques such as explicit or implicit schemes. The results obtained with the DAM are better than those obtained with such schemes for the following reasons:

the response with DAM is practically exact;

less time segments to find the response are necessary in comparison to the Newmark-β method;

no aliasing phenomenon exists with DAM;

the time segment is automatically estimated by the algorithm without any user input except for the tolerance ε (equation 18).

Since the DAM is in the family of explicit methods, stability is conditional and it depends on the value of the lowest period of vibration. Just as it is the case for the explicit central difference technique, the DAM can be combined with a mode superposition technique. In this case, the DAM is applied to each uncoupled equation (MDAM). Very good results were obtained with this method. One also observes, from example 5.2, that the CPU time requirements decrease as a function of the order N. Thus, it is better to use higher asymptotic developments.

The applications of the DAM have been presented for constant and cosine loads. The DAM can be used for other types of loading if the load vector is developed in a polynomial series as a function of time. This method can also be used for earthquake analysis using accelerograms with a linear approximation of the acceleration between two recorded acceleration values. The size of the time segment is then conditioned by the one used for the data acquisition of the accelerogram.

The DAM can be extended to the non-linear dynamic problem as well as to transient heat transfer by conduction [20]. In the latter case, the differential equation of the spatial discretization can be written as

$$[\mathbf{C}]\{\dot{\mathbf{T}}(t)\} + [\mathbf{K}]\{\mathbf{T}(t)\} = \{\mathbf{F}(t)\}$$

and the solution can be determined by the asymptotic method in terms of the following polynomial series:

$$\{\mathbf{T}(t)\} = \sum_{j=0}^{N} (t^j\{\mathbf{T}_j\}).$$

From the above discussion and conclusions, it is observed that the asymptotic method can be considered as a general quasi-analytical method. For a partial differential equation in time and space domain, the space can be discretized using the finite element method. The remaining system of equations becomes a set of ordinary differential equations. It is obvious that, if the load vector is defined in a polynomial form, the application of the asymptotic method to solve the ordinary differential equation is similar to the method of undetermined coefficients. More detailed studies on the computational performances (memory and CPU time requirements) and the wide application of the DAM in comparison with the classical Euler explicit and Newmark-β schemes are under progress at Laval University [21].

ACKNOWLEDGMENTS

This research was funded by the National Sciences and Engineering Research Council of Canada and le Fonds FCAR from the Province of Quebec. The authors would like to acknowledge M. Eric Dionne from GIREF Laval University, for his contribution to this paper.

REFERENCES

1. C. Lanczos 1956 *Applied Analysis*. Englewood Cliffs, N.J.: Prentice Hall.
2. W. T. Koiter 1945 *On the stability of elastic equilibrium*. Ph.D. thesis, Delft, Netherlands. Translated by U.S. Air Force Dynamic Lab., Report AFF DL-TR-70-25.

3. J. M. T. THOMPSON and A. C. WALKER 1968 *International Journal of Solids and Structures* **14**, 757–768. The nonlinear perturbation analysis of discrete structural systems.
4. R. H. GALLAGHER 1975 *Computational Mechanics – Lecture Notes in Mathematics* **406**, 75–89. Berlin: Springer-Verlag. Perturbation procedures in nonlinear finite element structural analysis.
5. B. BUDIANSKY 1974 *Advances in Applied Mechanics* **14**, 1–65. Theory of buckling and post-buckling behavior of elastic structures.
6. M. POTIER-FERRY 1978 *Lecture Notes in Physics* **288**, 1–82. Foundations of elastic post-buckling theory.
7. N. DAMIL and M. POTIER-FERRY 1990 *International Journal of Engineering Sciences* **28**, 943–957. A new method to compute perturbed bifurcations: Application to buckling of imperfect elastic structures.
8. B. COCHELIN 1994 *Numerical asymptotic method for the geometrically nonlinear analysis of elastic structures*. Ph.D. thesis, University of Metz, France (in French).
9. B. COCHELIN, N. DAMIL and M. POTIER-FERRY 1994 *Computers and Structures* **53**, 1181–1192. A path following technique via an asymptotic-numerical method.
10. B. COCHELIN, N. DAMIL and M. POTIER-FERRY 1994 *Revue européenne des éléments finis* **3**, 281–297. The asymptotic-numerical method: an efficient perturbation technique for nonlinear structural mechanics.
11. B. COCHELIN, N. DAMIL and M. POTIER-FERRY 1994 *International Journal for Numerical Methods in Engineering* **37**, 1187–1213. Asymptotic-numerical methods and Padé approximants for non-linear elastic structures.
12. S. AMMAR 1996 *Perturbed asymptotic method applied to nonlinear problem with large rotations and large deformations* Ph.D. thesis, Department of Civil Eng., Laval University, Quebec, Canada (In French).
13. R. W. CLOUGH and J. PENZIEN 1993 *Dynamics of Structures*. New York: McGraw-Hill.
14. K. J. BATHE and E. I. WILSON 1976 *Numerical Methods in Finite Element Analysis*. New Jersey: Englewood Cliffs; Prentice-Hall.
15. P. V. O'Neil 1995 *Advanced Engineering Mathematics*, Boston: PWS-Kent, fourth edition.
16. E. KREYSZIG 1993 *Advanced Engineering Mathematics*, New York: MacGraw-Hill, Seventh edition.
17. T. J. R. HUGHES 1987 The finite element method, Englewood Cliffs: Prentice-Hall.
18. A. FILIATRAULT 1995 *Eléments de génie sismique*. Department of Civil Engineering, ecole Polytechnique de Montreal, Quebec, Canada (In French).
19. Y. H. LIN and M. W. TRETHEWEY *Journal of Sound and Vibration* **136**, 323–342. Finite element analysis of elastic beams subjected to moving dynamic loads.
20. G. GENDRON and M. FAFARD 1997 *Proceedings of the* 16*th Canadian Congress of Applied Mechanics* (*CANCAM*), June 1–5, 413–414. An asymptotic method for transient temperature calculations.
21. E. DIONNE 1997 *Asymptotic method applied to the time domain solution of equations of motion*. M.Sc. thesis, Department of Civil Eng., Laval University, Quebec, Canada (In French).

APPENDIX A: NOTATION

A_1, A_2	invariant of the amplification matrix
c	damping coefficient of the damper
$[\mathbf{C}]$	damping matrix
$f(t)$	non homogenous part of the differential equation
$\{\mathbf{F}(t)\}$	nodal load vector
$\{F_j\}$	nodal asymptotic load vectors
k	stiffness of a spring
$[\mathbf{K}]$	stiffness matrix
m	mass sustained by a spring
$[\mathbf{M}]$	mass matrix
N	maximum order of the asymptotic polynomial series
$[\mathbf{S}]$	amplification matrix
t	time
t_{crit}	critical time
u_h	complementary solution of a homogenous ordinary differential equation
u_p	particular solution of a non-homogenous ordinary differential equation
$\{\mathbf{u}(t)\}, \{\dot{\mathbf{u}}(t)\}, \{\ddot{\mathbf{u}}(t)\}$	nodal displacement, velocity and acceleration vectors

$\{\mathbf{u}^p(t)\}$ $\{\ddot{\mathbf{u}}^p(t)\}$	nodal displacement and velocity vectors at the end of time segment p
$\{\mathbf{u}^{p+1}(t)\}$ $\{\dot{\mathbf{u}}^{p+1}(t)\}$	nodal displacement and velocity vectors at the end of time segment $p+1$
$\{\mathbf{u}_0\}$	nodal initial displacement vector
$\{\mathbf{u}_1\}$	nodal initial velocity vector
$\{\mathbf{u}_j\}$	nodal vectors of the asymptotic development
$[\mathbf{X}]$	matrix of eigenvectors
$\{\mathbf{y}\}$	generalized displacement vector (in the modal space)
Δt	time step or time segment
ε	tolerance value to compute the critical time
$\lambda_{1,2}$	eigenvalues of the amplification matrix
$[\boldsymbol{\omega}^2]$	diagonal matrix with frequency values squared on the diagonal
ω	undamped natural frequency
ω_D	damped natural frequency
Ω	frequency of the exciting force
ρ	spectral radius of the amplification matrix
$[2\boldsymbol{\xi\omega}]$	diagonal damping matrix in the modal space
τ	interval of time starting at t^i_{crit}